

Los Alamos National Laboratory is operated by the University of California for the United States Department of Energy under contract W-7405-ENG-36.

---

**TITLE: POLARIZATION TRANSFER IN (p,n) REACTIONS AT 495 MeV**

**AUTHOR(S): T. N. Taddeucci**

1991

**SUBMITTED TO: The Proceedings of the 1991 International Conference on Spin and Isospin in Nuclear Interactions, Telluride, Colorado, March 11-15, 1991**

**DISCLAIMER**

This report was prepared as an account of work sponsored by an agency of the United States Government. Neither the United States Government nor any agency thereof, nor any of their employees, makes any warranty, express or implied, or assumes any legal liability or responsibility for the accuracy, completeness, or usefulness of any information, apparatus, product, or process disclosed, or represents that its use would not infringe privately owned rights. Reference herein to any specific commercial product, process, or service by trade name, trademark, manufacturer, or otherwise does not necessarily constitute or imply its endorsement, recommendation, or favoring by the United States Government or any agency thereof. The views and opinions of authors expressed herein do not necessarily state or reflect those of the United States Government or any agency thereof.

By acceptance of this article, the publisher recognizes that the U.S. Government retains a nonexclusive, royalty-free license to publish or reproduce the published form of this contribution, or to allow others to do so, for U.S. Government purposes.

The Los Alamos National Laboratory requests that the publisher identify this article as work performed under the auspices of the U.S. Department of Energy

---

**Los Alamos** Los Alamos National Laboratory  
Los Alamos, New Mexico 87545

## POLARIZATION TRANSFER IN (p,n) REACTIONS AT 495 MeV

T.N. Taddeucci

Los Alamos National Laboratory  
Los Alamos, NM 87545

### ABSTRACT

Polarization transfer observables have been measured with the NTOF facility at LAMPF for (p,n) reactions at 495 MeV. Measurements of the longitudinal polarization transfer parameter  $D_{LL}$  for transitions to discrete states at  $0^\circ$  show convincing evidence for tensor interaction effects. Complete sets of polarization transfer observables have been measured for quasifree (p,n) reactions on  $^2\text{H}$ ,  $^{12}\text{C}$ , and  $^{40}\text{Ca}$  at a scattering angle of  $18^\circ$ . These measurements show no evidence for an enhancement in the isovector spin longitudinal response.

### INTRODUCTION

The spin response probed by quasifree (p,n) reactions is of particular interest because of its relationship to the strength and momentum-transfer dependence of the residual isovector particle-hole interaction. Collectivity induced by this interaction is expected to produce significant differences between the isovector spin longitudinal ( $\vec{\sigma} \cdot \vec{q}$ ) and spin transverse ( $\vec{\sigma} \times \vec{q}$ ) responses at a momentum transfer of about  $1.75 \text{ fm}^{-1}$ .<sup>1</sup> In principle, the two responses can be experimentally distinguished by measuring complete sets of polarization transfer (PT) observables.<sup>2</sup>

The first measurement of the collective spin response induced by proton scattering involved  $(p,p')$  quasifree scattering at 500 MeV and  $18.5^\circ$ .<sup>2</sup> This measurement found no evidence for the expected enhancement of the longitudinal spin response with respect to the transverse spin response. However, a lingering source of uncertainty in interpreting the data is the mixed isoscalar and isovector nature of the  $(p,p')$  reaction. Ideally, this uncertainty is removed by repeating the experiment using the pure isovector  $(p,n)$  reaction.

Even with a pure isovector probe, however, additional uncertainties remain. One effect of great interest is the nature of the nucleon-nucleon interaction when embedded in the nuclear medium. Horowitz, Murdock, and Iqbal have used a Fermi-gas model of the nucleus to calculate the signatures for relativistic modifications of the interaction in quasifree scattering.<sup>3</sup> These signatures involve differences between the PT observables for quasifree scattering and those for free scattering. Collectivity in the nuclear response will also alter the PT observables, however. An obvious difficulty, then, is deciding whether to attribute observed differences between free and quasifree observables to a medium modification of the interaction or to collectivity in the nuclear response.

An alternate strategy for investigating the effective interaction is to make use of transitions to discrete states as a nuclear filter to isolate specific components of the interaction. In many cases spin and momentum transfer are the only important parameters involved and simple expressions can be derived for PT observables in terms of basic nucleon-nucleon amplitudes.<sup>4</sup>

In this article I will present new polarization transfer data for both discrete  $(p,n)$  transitions and for quasifree  $(p,n)$  scattering for a bombarding energy of 495 MeV. The data for discrete transitions involve the longitudinal polarization transfer parameter  $D_{LL}(0^\circ)$ . For quasifree scattering a complete set of PT observables has been obtained for  $^2\text{H}$ , C, and Ca. This latter set of measurements was obtained at the same bombarding energy and momentum transfer as the earlier  $(p,p')$  data<sup>2</sup> and provides the first look at the purely isovector spin responses induced by nucleon scattering.

## EXPERIMENTAL TECHNIQUE

The data presented here were obtained with the Neutron Time-of-Flight Facility (NTOF) at the Clinton P. Anderson Meson Physics Facility (LAMPF) in Los Alamos. The NTOF facility has been described briefly in previous conference proceedings.<sup>5</sup> Cross section and analyzing power data for (p,n) reactions were first obtained with this facility in 1987 with polarized beam provided by a Lamb-shift source. The recent commissioning of a new optically-pumped polarized ion source<sup>6</sup> (OPPIS) that can provide intense (100 nA) chopped (200 ns pulse spacing) polarized beam has made possible the first measurements of complete sets of polarization transfer observables for (p,n) reactions.

High-resolution measurements of polarization transfer in (p,n) reactions commenced at the Indiana University Cyclotron Facility (IUCF) in 1982, and many of the techniques developed there<sup>7</sup> have been scaled up and applied to the NTOF facility at LAMPF. The NTOF detector/polarimeter is illustrated schematically in Fig. 1. The detector consists of four parallel "planes" oriented perpendicular to the incident neutron flux: three stainless steel tanks filled with liquid scintillator (BC-517s, H:C=1.7) and a fourth set of ten plastic scintillators (BC-408). The liquid scintillator tanks are each subdivided into ten optically-isolated cells with dimensions of 10 cm  $\times$  10 cm  $\times$  107 cm. The plastic scintillator cells have the same dimensions. Thin plastic scintillators in front of and between the front and back pairs of neutron detectors are used to tag charged particles.

The front pair of planes serve as neutron polarization analyzers. Time, position, and pulse-height information from front and back planes are used to kinematically select n+p interactions. Neutron polarization is determined from the azimuthal intensity distribution of these events. Elastic  $^1\text{H}(n,n)$  and charge-exchange  $^1\text{H}(n,p)$  events are identified and sorted separately. Because of energy-resolution limitations in the interplane timing, quasifree n+C events also contribute to both of these reaction channels.

Incident neutron energy is determined by time of flight (TOF) to the front detector planes with respect to an rf stop signal derived from the linac. The neutron flight path varies according to resolution and count rate requirements. The range of possible values is 170 m to 620 m. Calibration measurements employing  $^{14}\text{C}$  were made on a 400 m-flight path with

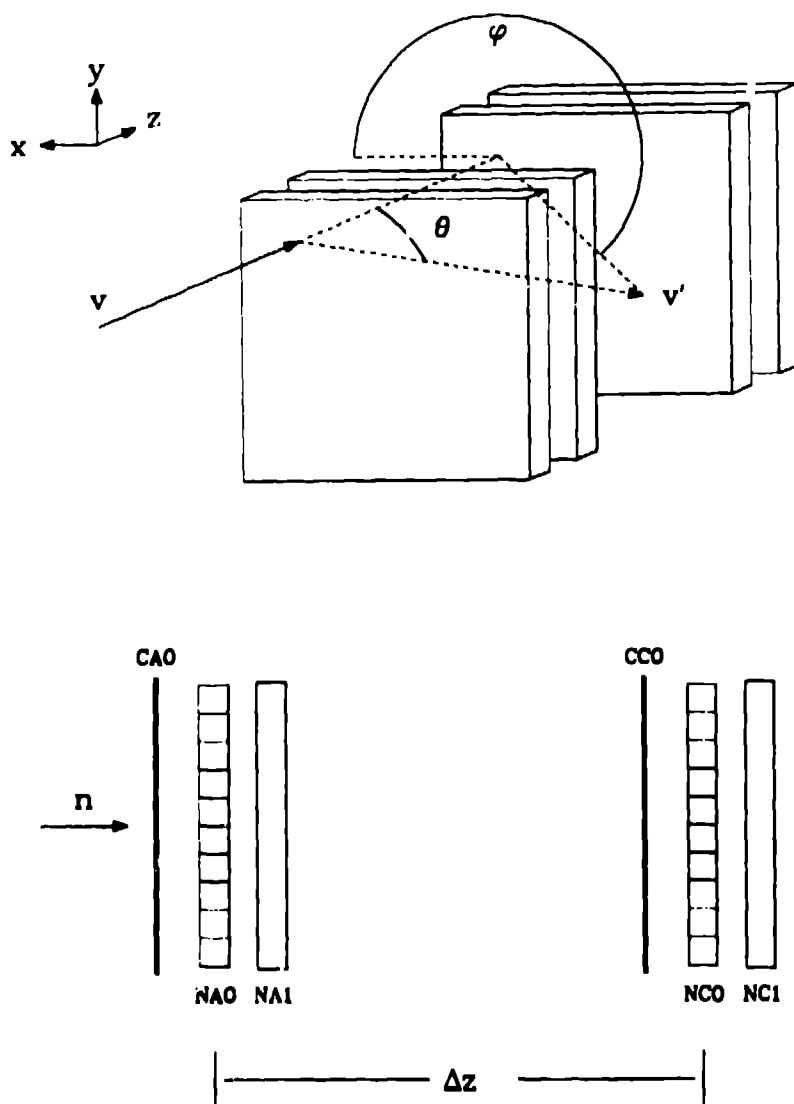


Fig. 1. The NTOF neutron polarimeter. The front detector planes (NAO,NA1) serve as polarization analyzers and are separated from the two back planes (NCO,NC1) by an average separation of  $\Delta z=1.7$  m. Two sets of thin scintillators (CAO,CCO) are used to tag charged particles.

an average energy resolution of about 0.75 MeV at a bombarding energy of 495 MeV. The best resolution obtained at this flight path was 0.6 MeV. The measurements of quasifree polarization transfer were made on a flight path of 200 m. In both cases time and energy spread in the beam were minimized with a rebunching technique that employs nonaccelerating rf cavities in the linac.<sup>8</sup>

The beam intensity and polarization for the present measurements were typically 70 nA and 55%. Nominal beam energy was 495 MeV. With the thick targets (1 g/cm<sup>2</sup>) used in the quasifree measurements, approximately one day

of beam on target was required for each incident polarization state per target.

The effective analyzing power for each reaction channel in the polarimeter has been determined by observing neutrons produced by the  $^{14}\text{C}(\text{p},\text{n})^{14}\text{N}(2.31\text{-MeV})$  reaction. For this  $0^+ \rightarrow 0^+$  transition, outgoing neutrons at a scattering angle of  $0^\circ$  have the same polarization as the incident proton beam. A spectrum for the  $^{14}\text{C}(\text{p},\text{n})$  reaction at 495 MeV is shown in Fig. 2. This measurement employed longitudinally polarized beam.

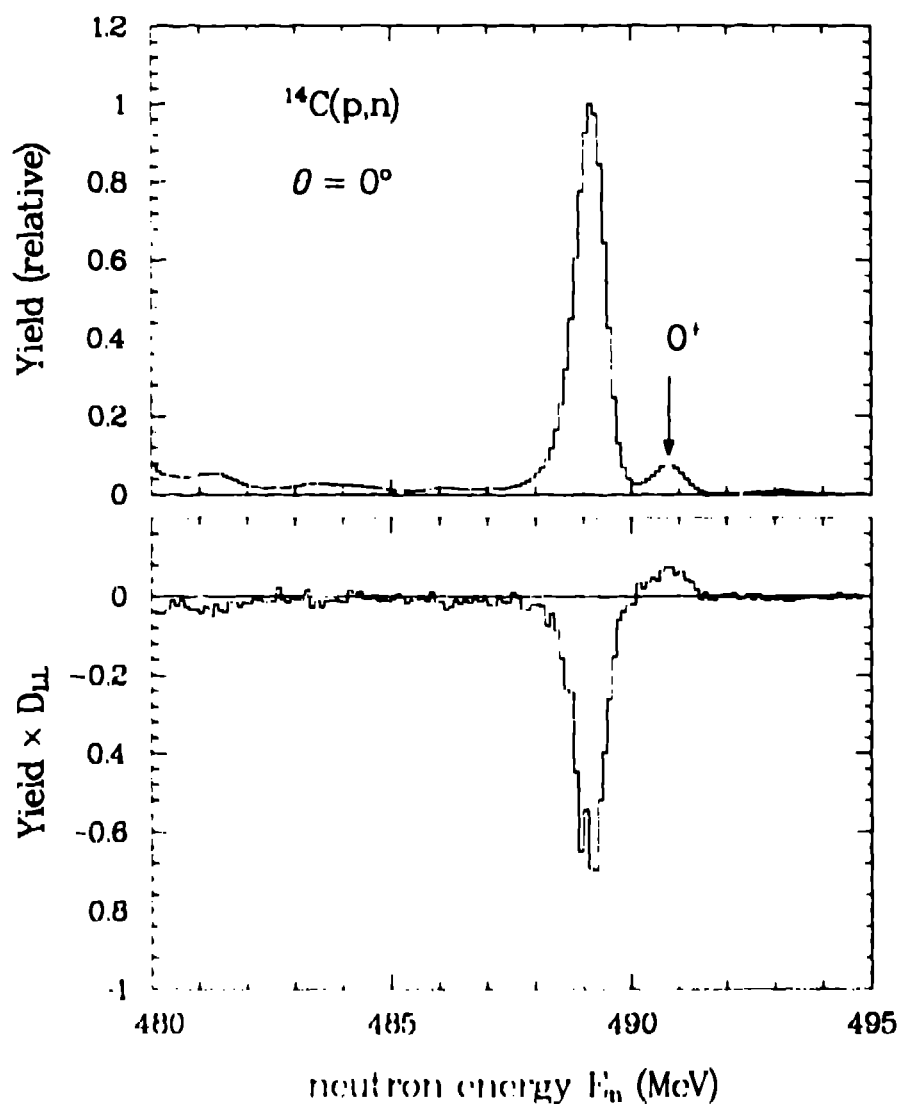


Fig. 2. Spectrum for the  $^{14}\text{C}(\text{p},\text{n})$  reaction at 495 MeV. Neutrons from the transition to the  $0^+$  isobaric analog state at 2.31 MeV are used to calibrate the polarimeter.

Horizontal and vertical dipole magnets were used to precess the outgoing L-type polarization into equal N and S components at the detector.

Two different precession schemes are used to measure polarization transfer observables at nonzero angles. For sideways (S) and longitudinally (L) polarized beams, a horizontal dipole field is used to precess the outgoing L component into N (normal to reaction plane) polarization at the detector. The outgoing S polarization is unaffected by this field, while the induced N-type polarization is precessed into L polarization at the detector. Because the induced N-type polarization is now unobservable, reversal of the proton polarization also reverses the observable components of neutron polarization incident on the detector. This reversal allows cancellation of instrumental asymmetries. For measurements with N-type beam, the horizontal dipole field is reduced for minimum precession effect (it cannot be turned off because this magnet also functions as a sweep magnet) and a superconducting solenoid is used to precess the outgoing N type polarization alternately by  $\pm 90^\circ$ . These reversals are again necessary for cancellation of instrumental asymmetries.

#### ZERO-DEGREE SCATTERING AND THE TENSOR EXCHANGE INTERACTION

At sufficiently high bombarding energy ( $E_p > 100$  MeV) and at low momentum transfer ( $\theta = 0^\circ$ ), the spectrum of final states excited in (p,n) reactions is dominated by  $\Delta J^\pi = 1^+$  transitions. These transitions involve the same matrix elements that apply in beta decay, but without the binding-energy restrictions that limit actual beta decays to transitions between only a few low-lying levels. To the extent that the (p,n) transitions are pure  $\Delta L = 0$  and are mediated by the central interaction only, a direct connection can be made between the (p,n) cross sections and the corresponding beta-decay transition strengths. Polarization transfer provides a sensitive means of testing for the presence of  $\Delta L > 0$  and noncentral amplitudes.

The plane-waves impulse approximation (PWIA), coupled with simplifying nuclear-structure assumptions, allows polarization transfer coefficients to be expressed in terms of free nucleon nucleon amplitudes.<sup>4</sup> Much of the utility of polarization transfer derives from the applicability of these simple expressions. A common form for the nucleon nucleon scattering matrix is

$$M = A + C(\sigma_{1n} + \sigma_{2n}) + B\sigma_{1n}\sigma_{2n} + E\sigma_{1q}\sigma_{2q} + F\sigma_{1p}\sigma_{2p} \quad (1)$$

or, after rearranging terms

$$M = A + C(\sigma_{1n} + \sigma_{2n}) + \frac{1}{3}(B+E+F)\vec{\sigma}_1 \cdot \vec{\sigma}_2 + \frac{1}{3}(E-B)S_{12}(\hat{q}) + \frac{1}{3}(F-B)S_{12}(\hat{p}). \quad (2)$$

Here, the coordinates  $\hat{q} = \vec{k}_f - \vec{k}_i$ ,  $\hat{n} = \vec{k}_i \times \vec{k}_f$ , and  $\hat{p} = \hat{q} \times \hat{n}$  are defined in terms of the initial and final momenta  $k_i$  and  $k_f$ ;  $S_{12}$  is the tensor operator. The coefficients in Eqs. (1) and (2) can be subdivided into isoscalar and isovector components. In the following discussion, isovector terms are assumed.

The first four combinations of amplitudes in Eq. (2) can be identified with the familiar t-matrix interaction amplitudes  $V_T$ ,  $V_{LS}$ ,  $V_{ST}$ , and  $V_{TT}$ . The fifth term in Eq. (2) has no direct analog in local t-matrix parametrizations; it is, instead, approximated by the tensor exchange amplitude.

At a scattering angle of  $0^\circ$  there are only two unique polarization transfer coefficients:  $D_{NN}$  and  $D_{LL}$ . Furthermore, if the spin and parity of the transition is well-defined these two coefficients are not independent but are related by the expression

$$D_{NN} = \pm \frac{1}{2}(1 + D_{LL}), \quad (3)$$

where the plus sign applies for natural parity transitions ( $0^+, 1^-, \dots$ ) and the minus sign applies for unnatural parity transitions ( $0^-, 1^+, \dots$ ). The N-N scattering matrix simplifies at  $\Theta=0^\circ$ , where  $E=B$  and  $C=0$ . The general expression for the polarization transfer coefficient  $D_{NN}$  for pure  $\Delta L=0, 1^+$  transitions then becomes<sup>4</sup>

$$D_{NN}(0^\circ, 1^+) = \frac{F^2}{2B^2 + F^2}. \quad (4)$$

If the exchange tensor amplitude is negligible,  $B \approx F$ , then



$$D_{NN}(0^\circ, 1^+, \text{central}) = -\frac{1}{3}. \quad (5)$$

Deviations from this "ideal" value therefore signal the presence of noncentral or  $\Delta L > 0$  amplitudes. Many  $1^+$  transitions have been observed at IUCF in the energy range 120–200 MeV. Individual data points are displayed in Fig. 6 of Ref. 9. The average empirical value for  $1^+$  transitions in this energy range is  $D_{NN}(0^\circ) = -0.33 \pm 0.05$ .

There is no fundamental reason for the exchange tensor amplitude to be negligible at small momentum transfer. Indeed, it is interesting to employ Eq. (4) and the free N-N amplitudes to map out the expected value of  $D_{NN}$  as a function of bombarding energy. This is done in Fig. 3. The solid data points plotted in this figure represent measured values for the  $^{14}\text{C}(p,n)^{14}\text{N}(3.95\text{-MeV})$  transition. The 120 MeV and 160 MeV points ( $D_{NN}$ ) were obtained at IUCF. The 495 MeV point ( $D_{LL}$  converted to  $D_{NN}$ ) was obtained recently at LAMPF. The thick hashed line represents the prediction of Eq. (4). Amplitudes were obtained from the SM89 phase-shift solution of Arndt.<sup>11</sup> The thin lines represent plane-waves calculations for several p-shell single-particle transitions in carbon, calculated with the code DWBA80<sup>11</sup> and the t-matrix interaction of Franey and Love.<sup>12</sup>

The t-matrix calculations and Eq. (4) both give the same general energy trend. In the IUCF energy range the t-matrix values are comfortably close to the measured values, while the N-N amplitude values are too negative. Near 500 MeV, the  $^{14}\text{C}$  measurement is better described by the simple N-N amplitude expression. Comparisons such as those in Fig. 3 can emphasize specific deficiencies in the interaction parameters, in this case the tensor (exchange) interaction, or alternately, indicate energy regions in which simple impulse approximation expressions such as Eq. (4) are less accurate than reaction-model calculations that better incorporate the off-shell nature of the interaction in the nuclear medium.

The  $^2\text{H}(p,n)^2\text{p}$  reaction represents a case for which there is minimal nuclear-medium modification of the interaction. In this reaction, at  $0^\circ$  the two residual protons are forced by the Pauli principle to be in a relative S-state ( $^1S_0$ ) when the momentum transfer is small. For small energy loss, the transition can therefore be characterized as  $1^+ \rightarrow 0^+$ , and Eq. (4) will

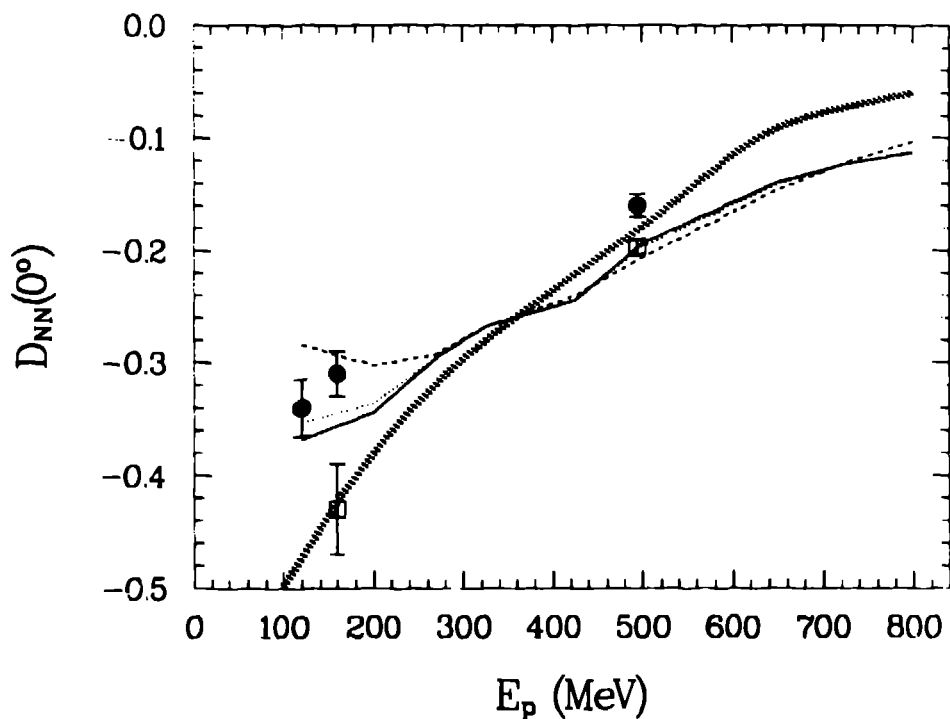


Fig. 3. Polarization transfer coefficient  $D_{NN}(0^\circ)$  for  $\Delta J^\pi=1^+$  transitions. The solid data points are for the  $^{14}\text{C}(p,n)^{14}\text{N}(3.95\text{-MeV})$  transition. The open boxes correspond to  $^2\text{H}(p,n)$ . The broad dashed line is calculated from N-N amplitudes and Eq. (4). The thin lines correspond to different single-particle transitions in carbon, calculated with a distorted-waves reaction code with the optical potential set to zero.

apply. Two measured values for the polarization transfer for this reaction (open boxes) are displayed in Fig. 3. The 160 MeV datum is a  $D_{NN}$  measurement.<sup>13</sup> The 495-MeV datum is  $D_{LL}$  converted to  $D_{NN}$ . Both of these data points correspond to a narrow interval (2-4 MeV wide) centered on the peak of the  $0^\circ$  distribution. The agreement between the  $^2\text{H}(p,n)$  measurements and the phase-shift predictions is very good. The  $0^\circ$  spectrum for this reaction at 495 MeV is displayed in Fig. 4. This figure shows that the polarization transfer varies with energy loss. This dependence arises from the contribution of  $\Delta L=1$  ( $^3\text{P}_{0,1,2}$ ) amplitudes to the zero degree scattering. The narrow energy interval employed for the above comparison was deliberately chosen to minimize these contributions.

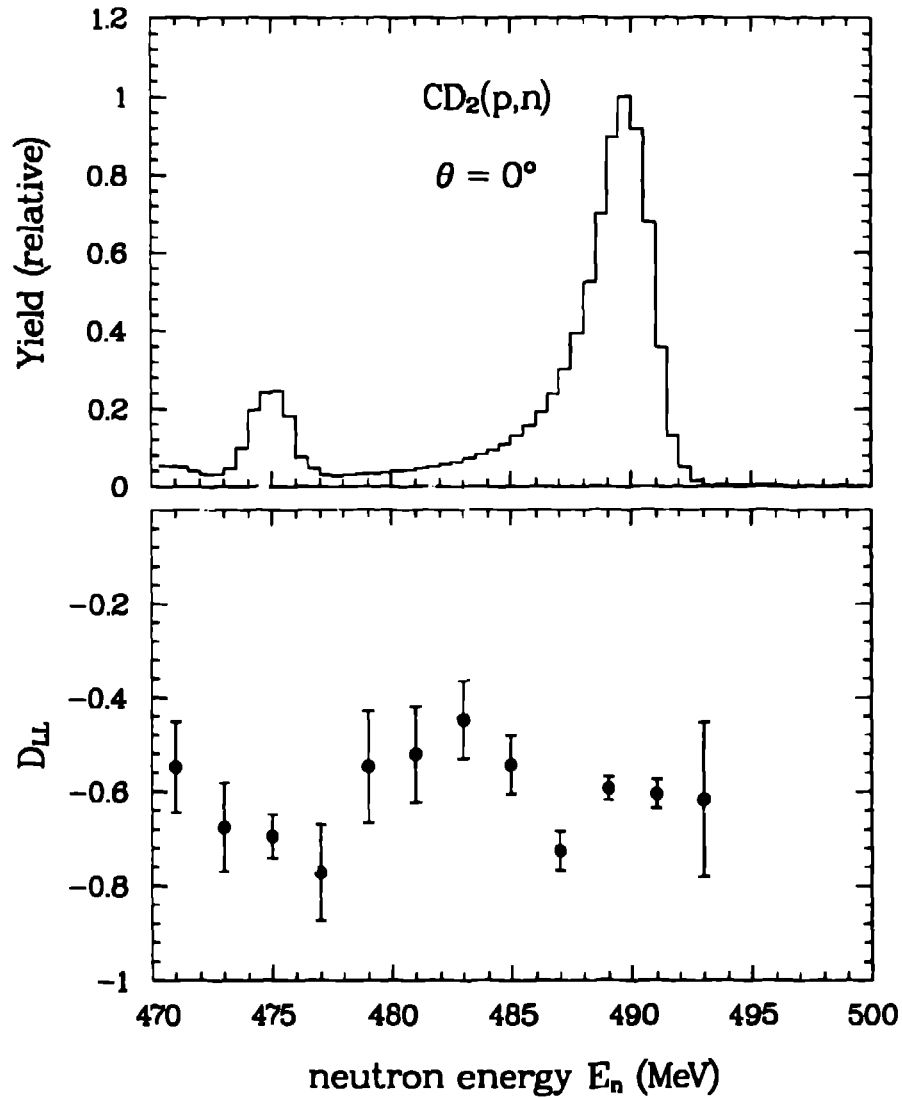


Fig. 4. Spectrum for  ${}^2\text{H}(p,n)$  at 495 MeV. The peak at  $E_n=475$  MeV is the  ${}^{12}\text{C}(p,n){}^{12}\text{N}(\text{g.s.})$  transition from the carbon content of the  $\text{CD}_2$  target.

The data and calculations presented here show quite clearly that  $\Delta J^\pi=1^+$  transitions do not have a unique energy-independent polarization transfer signature. Rather, the observed value of  $D_{NN}(0^\circ)$  [or  $D_{LL}(0^\circ)$ ] depends sensitively on the relative strengths of the central and tensor interactions. In the energy region accessible at IUCF (100-200 MeV) the effective tensor exchange contribution is very small in target nuclei heavier than  ${}^2\text{H}$  and  $1^+$  transitions have a PT signature characteristic of a purely central interaction. At LAMPF energies (200-800 MeV), however, the tensor exchange interaction has a significant effect on PT observables at

0°. A related question that has not yet been systematically addressed is how much of an effect this interaction has on the 0° cross sections for the higher bombarding-energy region. The answer to this question has obvious implications with regard to the choice of bombarding energy for studying 1<sup>+</sup> strength distributions.

#### QUASIFREE SCATTERING AND THE NUCLEAR SPIN RESPONSE

In the simplest model of quasifree scattering the projectile nucleon undergoes a single hard collision with a target nucleon and ejects it into the continuum. The remaining A-1 target nucleons act as spectators and do not participate in the reaction. The observables for this process should look very much like those for free scattering, except for differences arising from the Fermi motion of the struck nucleon.

Absorptive corrections to this simple model localize the interaction region to near the nuclear surface. Additional corrections include nuclear-medium modification of the interaction between the projectile and target nucleon, and inclusion of the nuclear collective response. In the latter case the remaining A-1 target nucleons are not simple spectators (i.e., a free Fermi gas), but rather participate in the reaction through the influence of the residual particle-hole interaction.

The simplest observable that can be calculated in the simple model is the position of the quasifree "peak". Using nonrelativistic kinematics, it is easy to show that the energy loss  $\omega$  of the projectile is given by

$$\omega = \frac{q^2}{2m} + \frac{\vec{p} \cdot \vec{q}}{m} + \frac{A}{A-1} \frac{p^2}{2m} - Q + \langle E_x \rangle \quad (6)$$

where  $q$  is the momentum transfer,  $p$  is the Fermi momentum of the struck target nucleon,  $Q$  is the reaction  $Q$ -value for ejecting a nucleon into the continuum, and  $\langle E_x \rangle$  is the average excitation energy of the residual A-1 nucleons. The first term is the energy loss for free scattering, the second term describes the width of the distribution arising from the Fermi motion of the struck nucleon, and the remaining terms represent a binding-energy shift in the position of this distribution. This shift should typically be of the order of 10-20 MeV. For example, the reaction  $Q$ -values for the

ejection of one neutron or one proton from  $^{12}\text{C}$  are  $Q_{pn} = -17.6$  MeV and  $Q_{pp} = -15.7$  MeV, respectively.

A good example of the (p,n) quasifree distribution is presented in Fig. 5. This figure shows the spectrum for  $^{12}\text{C}(p,n)$  at  $E_p = 795$  MeV and several different scattering angles. As expected, the width of the distribution increases with angle (increasing momentum transfer) and the centroid of the distribution is shifted by about 25 MeV with respect to the energy loss for free scattering (marked by vertical dashed lines).

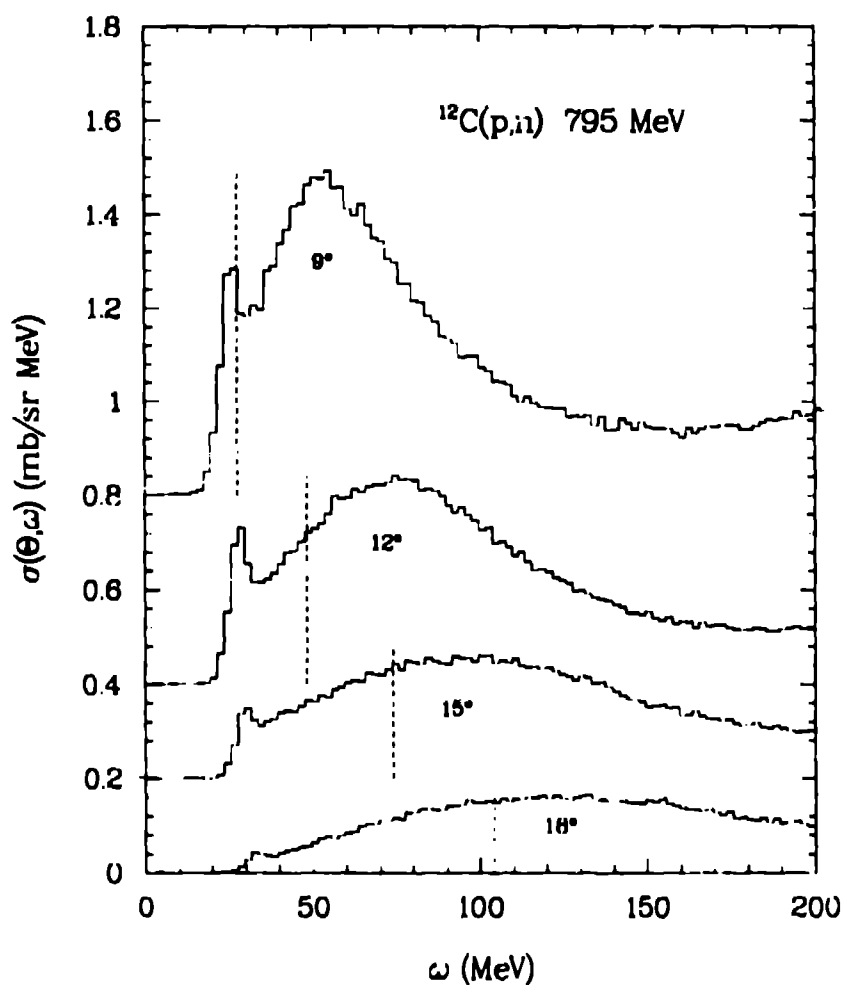


Fig. 5. Spectra for  $^{12}\text{C}(p,n)$  at 795 MeV. The dashed vertical lines mark the energy loss for free scattering. Cross section normalization is uncertain by about 20%.

A similar picture for  $(p,p')$  quasifree scattering is presented in Fig. 6. Here the data are from the work of Chrien et al.,<sup>14</sup> and show  $^{12}\text{C}(p,p')$  spectra for  $E_p = 795$  MeV and several angles. An immediate difference is evident when compared to the  $(p,n)$  spectra in Fig. 5. The location of the  $(p,p')$  quasifree peak is very nearly consistent with the energy loss for free scattering, and therefore inconsistent with Eq. (6) and the  $(p,n)$  data. A possible explanation for this difference is collectivity in the isoscalar response excited by the  $(p,p')$  reaction. Collectivity in the isoscalar channel [absent in  $(p,n)$ ] would enhance the response at low energy loss<sup>15,16</sup> and shift the centroid of the quasifree distribution toward low  $\omega$ . It should be noted that corrections for the isoscalar component in

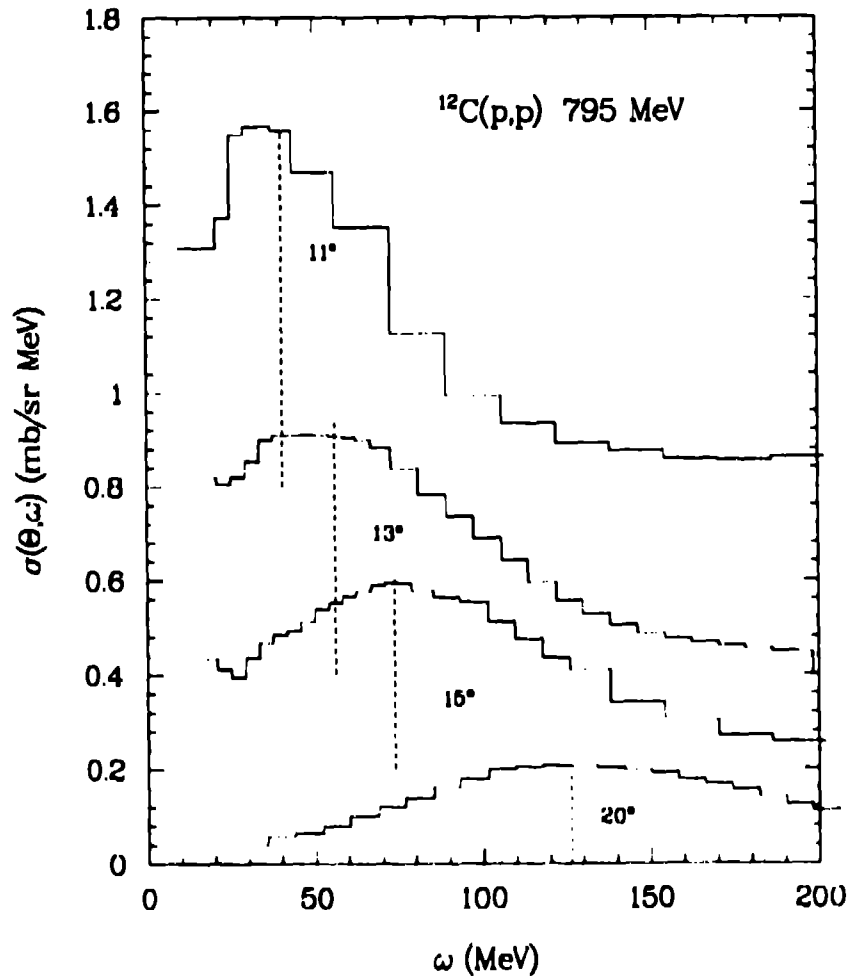


Fig. 6. Spectra for  $^{12}\text{C}(p,p')$  at 795 MeV. The dashed vertical lines are positioned at the energy loss for free scattering. Data are from the tables in Ref. 14.

the (p,p') PT transfer data explicitly assumed no collectivity in the isoscalar channel.<sup>2</sup>

The simplest spin observable to measure is the analyzing power. An additional difference between (p,n) and (p,p') quasifree scattering can be seen in the data for this observable. Figure 7 presents cross section and analyzing power spectra for (p,n) quasifree scattering on  $^2\text{H}$ ,  $^{12}\text{C}$ , and  $^{40}\text{Ca}$  for  $E_p = 495$  MeV and  $\theta_{\text{lab}} = 18^\circ$ . The analyzing power for  $^2\text{H}(p,n)$  is consistent with the free value, which is indicated by the solid horizontal line. The  $^{12}\text{C}$  and  $^{40}\text{Ca}$  data are either consistent with or slightly larger than the free value.

It is well known that the analyzing power for (p,p') quasifree scattering is substantially reduced with respect to free scattering.<sup>3,17</sup> This reduction has been attributed to a sensitive cancellation between the large scalar and vector potentials that apply in relativistic models of this reaction.<sup>3</sup> For (p,n) quasifree scattering there is only a single dominant term in the relativistic parametrization of the interaction. According to whether this term is parametrized as a pseudoscalar or pseudovector invariant, the analyzing power for (p,n) is predicted to be slightly smaller or larger than the free value, respectively.<sup>3</sup> The data presented in Fig. 7 would seem to favor the pseudovector parametrization, but the differences are small enough that distortion effects must also be considered.

The relativistic effects predicted for PT observables for (p,n) quasifree scattering at 500 MeV and  $\theta = 18^\circ$  are rather small.<sup>3</sup> If the pseudovector parametrization is assumed, the largest differences will occur in the coefficients  $D_{NN}$  and  $D_{SS}$ . An increase of about +0.1 with respect to the free value is predicted for  $D_{NN}$ , while a decrease of about the same amount is predicted for  $D_{SS}$ . The new (p,n) data, presented in Fig. 8, do not show any significant changes in the PT observables with respect to free scattering. Because of the ambiguities in the relativistic parametrization, a more conclusive test of this model will likely require comparison to data at several momentum transfers.

The diagonal PT coefficients  $D_{SS}$ ,  $D_{NN}$ , and  $D_{LL}$  are shown in Fig. 8. The data were obtained at 495 MeV and  $\theta_{\text{lab}} = 18^\circ$ . The momentum transfer is approximately  $1.72 \text{ fm}^{-1}$ . The  $^2\text{H}(p,n)$  data, displayed separately from the  $^{12}\text{C}$  and  $^{40}\text{Ca}$  data, were obtained with a  $\text{CD}_2$  target. A careful  $\text{CD}_2$  C subtraction yielded the  $^2\text{H}$  results. The free scattering value for each

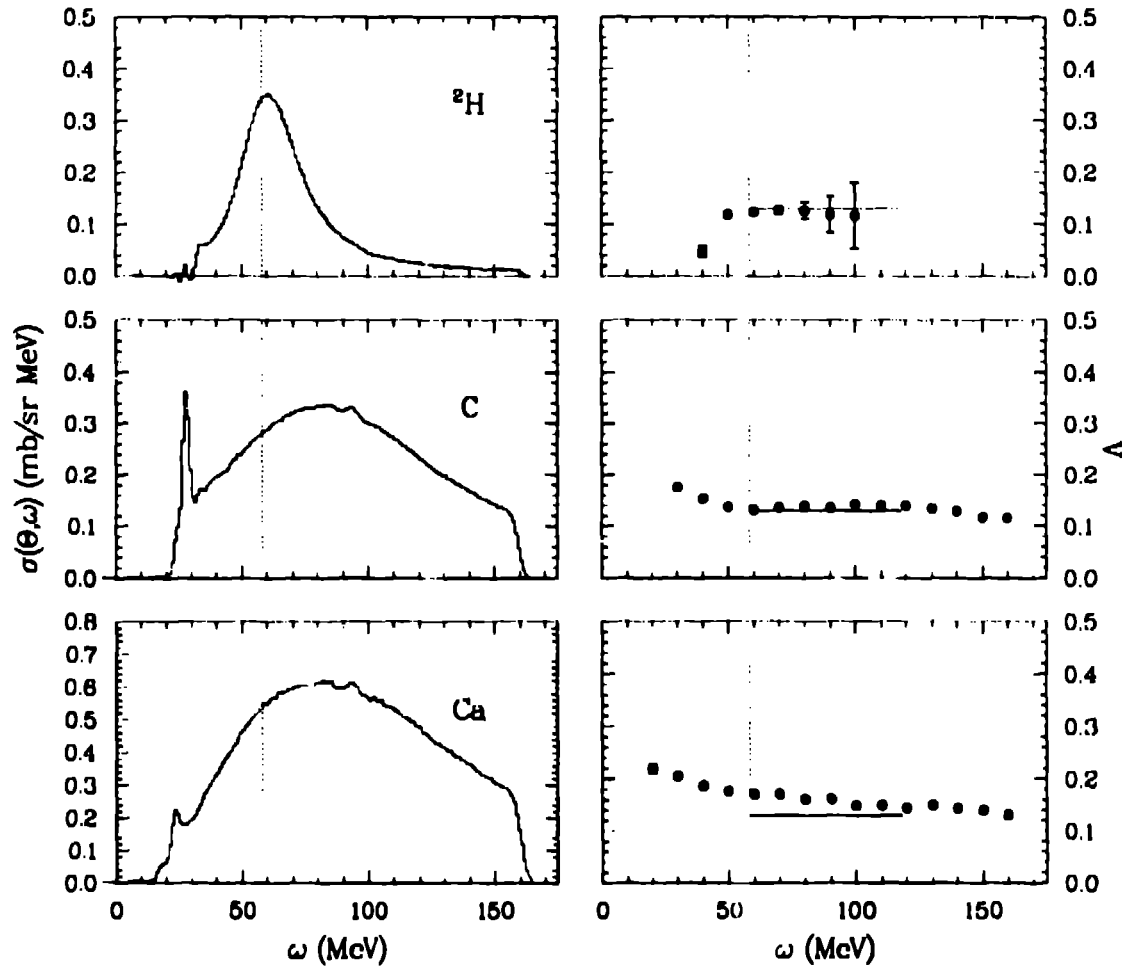


Fig. 7. Cross section and analyzing power for (p,n) reactions on  $^2\text{H}$ ,  $^{12}\text{C}$ , and  $^{40}\text{Ca}$  at 495 MeV and  $\theta_{\text{lab}} = 18^\circ$ . The dashed vertical line in each panel marks the energy loss for free scattering. The analyzing power for free scattering (from N-N phase shifts) is plotted as a solid horizontal line. A vestige of the two-proton final-state interaction can be seen at approximately 31 MeV in the  $^2\text{H}$  spectrum.

coefficient is displayed as a solid horizontal line in each panel. These values are obtained from the recent SM91 phase-shift solution of Arndt.<sup>10</sup> The  $^2\text{H}$  data should be regarded as the best representation of free scattering; the phase-shift values are merely shown for reference.

It is clear from Fig. 8 that there is little difference between the quasifree polarization transfer for  $^{12}\text{C}$  and  $^{40}\text{Ca}$  and that for free scattering, as represented by the  $^2\text{H}(p,n)$  data. With regard to collectivity in the nuclear spin response, the sought after signature is a ratio of



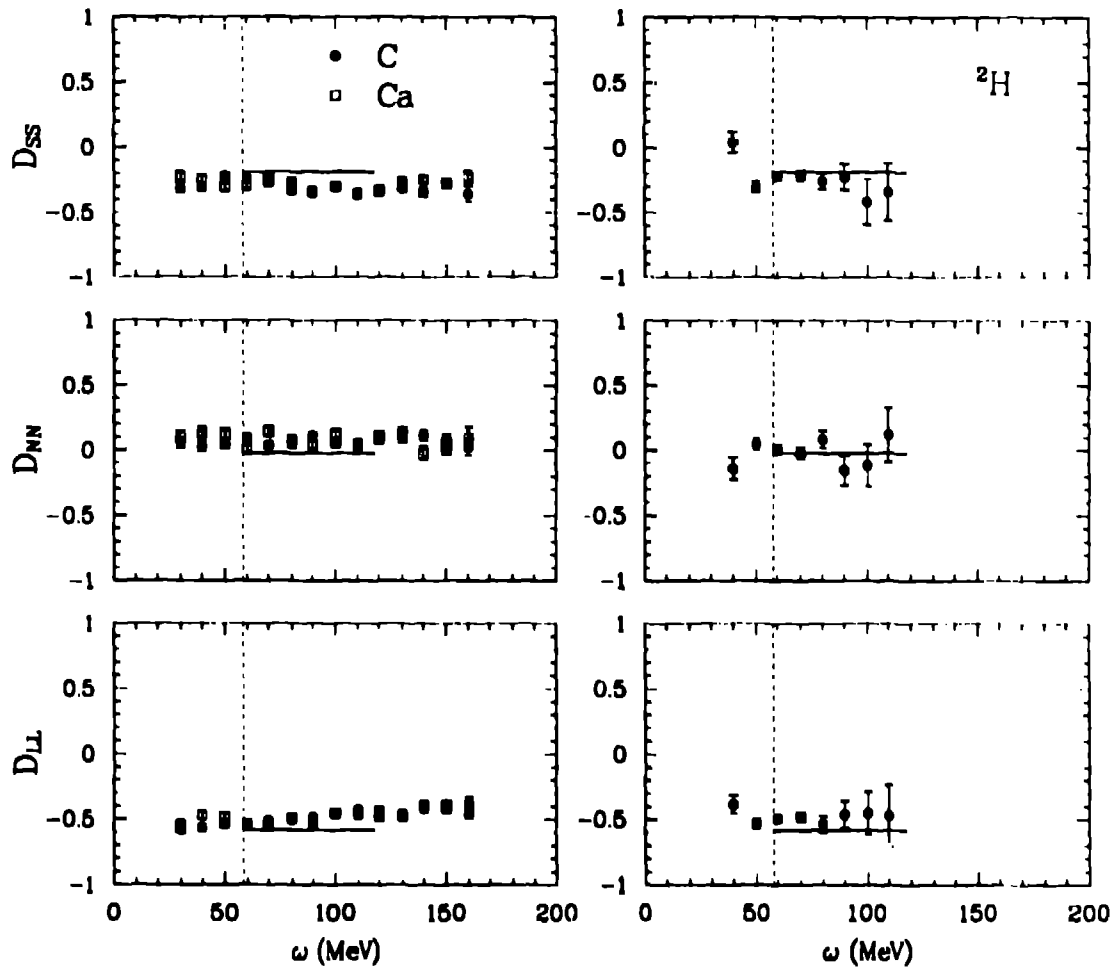


Fig. 8. Polarization transfer coefficients for (p,n) reactions on  $^2\text{H}$  (right) and  $^{12}\text{C}$  and  $^{40}\text{Ca}$  (left) at 495 MeV and  $\theta_{\text{lab}} = 18^\circ$ . Free-scattering values obtained from the Arndt SM91 phase-shift solution (Ref. 10) are shown as solid horizontal lines. Dashed vertical lines mark the energy loss for free scattering. These data are preliminary and are subject to an energy-dependent normalization uncertainty of about 10%.

longitudinal to transverse spin-flip probabilities that is different from the ratio for free scattering. If the longitudinal response is collectively enhanced relative to the transverse response, this ratio should be larger than unity. The longitudinal and transverse spin flip probabilities are defined by<sup>2</sup>

$$S_L = \frac{1}{4} [1 + D_{NN} + (D_{SS} - D_{LL}) \sec \theta_{\text{lab}}] \quad (7)$$

and

$$S_T = \frac{1}{4}[1 - D_{NN} - (D_{SS} - D_{LL})\sec\theta_{lab}]. \quad (8)$$

For free scattering, the ratio of these two quantities gives the ratio of the longitudinal and transverse amplitudes [Eq. (1)],

$$\frac{S_L}{S_T} = \frac{E^2}{F^2}. \quad (9)$$

In the static PWIA, this ratio for quasifree scattering yields a ratio of effective nucleon-nucleon amplitudes times the ratio of longitudinal ( $\vec{\sigma} \cdot \vec{q}$ ) and transverse ( $\vec{\sigma} \times \vec{q}$ ) responses:

$$\frac{S_L}{S_T} = \frac{E^2}{F^2} \frac{R_L}{R_T}. \quad (10)$$

If the ratio of effective amplitudes is the same as the ratio of free amplitudes, then Eq. (10) divided by Eq. (9) yields the ratio of nuclear spin responses:

$$\frac{(S_L/S_T)_A}{(S_L/S_T)_D} = \frac{R_L}{R_T}, \quad (11)$$

where A refers to the quasifree ratio for nuclide A and D refers to the deuterium ratio.

The ratio of longitudinal and transverse spinflip probabilities for deuterium is presented in Fig. 9. The solid horizontal line represents the free nucleon nucleon value from the SM91 phase-shift solution. As an indication of how stable the phase-shift solutions have been, the SM86 value is plotted on this figure as a dotted line, and the SM90 value as a dashed line.

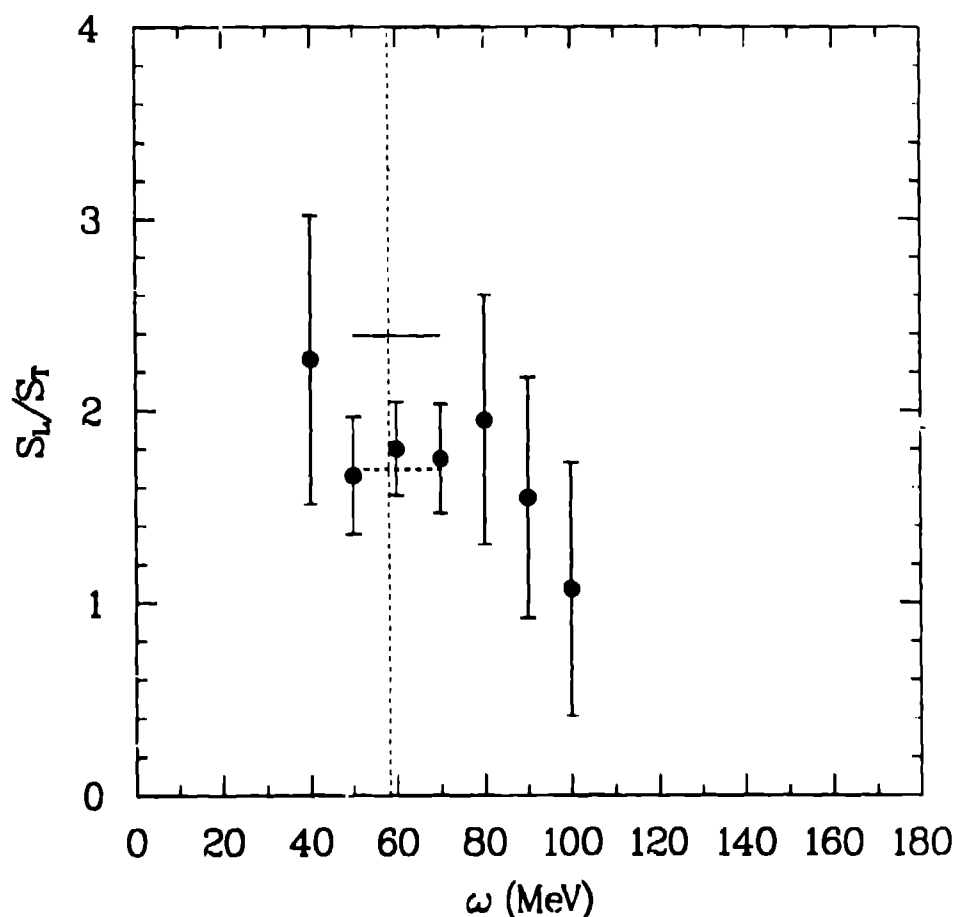


Fig. 9. Ratio of the longitudinal and transverse spinflip probabilities for  $^2\text{H}(p,n)$  at 495 MeV and  $\theta_{\text{lab}} = 18^\circ$ . The ratios obtained from N-N phase shifts (Ref. 10) are: SM86 (dotted), SM90 (dash), SM91 (solid).

The super ratio defined in Eq. (11) is plotted for  $^{12}\text{C}$  and  $^{40}\text{Ca}$  in Fig. 10. The (p,n) results obtained here are very similar to the earlier (p,p') results. The ratio is everywhere consistent with unity or somewhat smaller. The expected longitudinal enhancement is not seen. The results for  $^{12}\text{C}$  and  $^{40}\text{Ca}$  are very similar and suggest that choice of target nuclide is not very important. This similarity is not too surprising in view of the surface-peaked nature of the reaction.<sup>2</sup>

Several effects may conspire to suppress the expected longitudinal/transverse enhancement as seen in the experimental ratio. In the surface region, decreased nuclear density and mixing between the longitudinal and transverse modes will both diminish the expected signature.

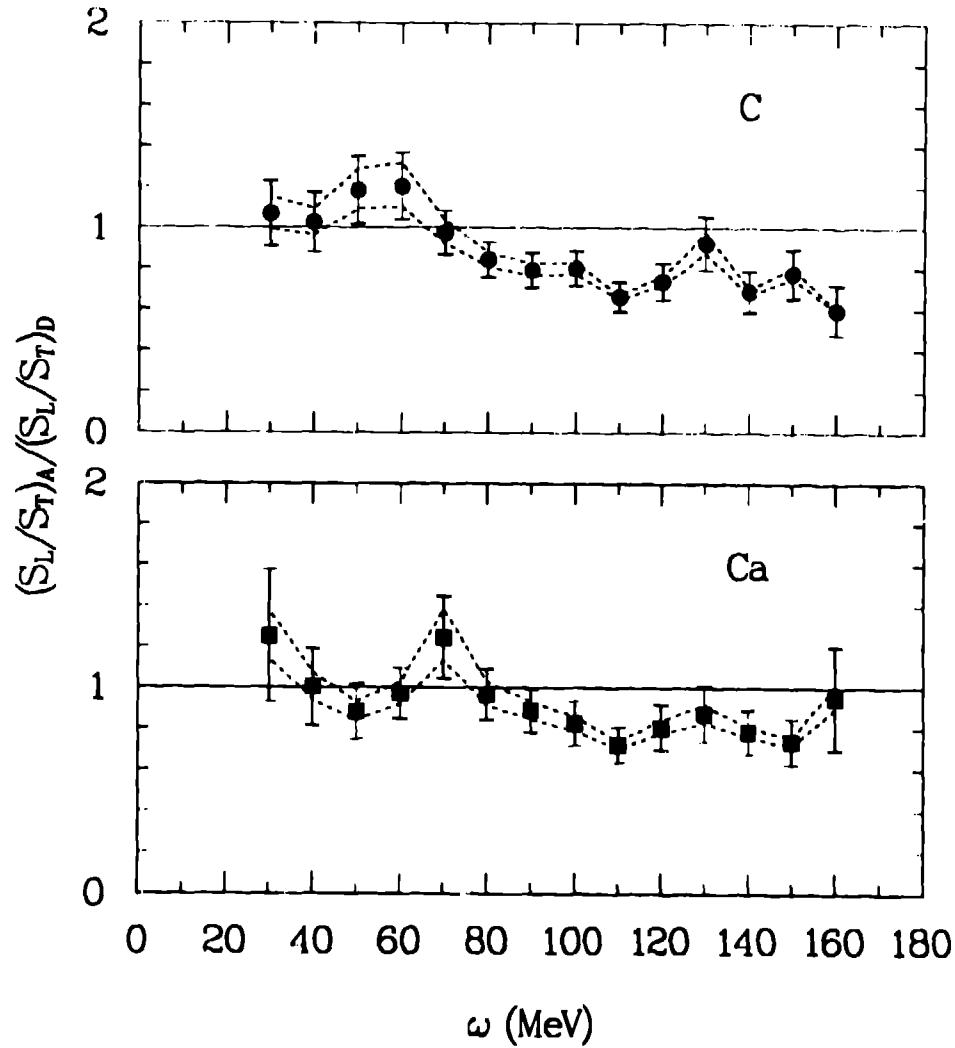


Fig. 10. Longitudinal/transverse spinflip ratios for carbon and calcium divided by the ratio for deuterium. This "super-ratio" should closely approximate the ratio of longitudinal and transverse spin responses. The dashed lines represent the error bounds on the data corresponding to a  $\pm 10\%$  normalization uncertainty in the polarization transfer measurements.

Distortion effects must also be considered. What is needed is a calculation that combines both nuclear structure and reaction dynamics in a realistic way. Ichimura et al. have performed distorted-waves RPA calculations in a study of the  $(p,p')$  data,<sup>16</sup> and are currently producing new calculations for the  $(p,n)$  case.<sup>19</sup> The preliminary conclusion to be drawn from the new calculations is that the theoretical ratio is still too large in the low- $\omega$  region, and best consistency with the data is obtained when the RPA correlations are turned off. This is a surprising result, and may indicate a problem with the assumed form of the residual particle hole interaction.

Additional experimental data at different momentum transfers will help to understand this problem. Such measurements are already planned.

#### ACKNOWLEDGEMENTS

Many people have contributed to the effort that produced the data in this article. They are: T.A. Carey, J.B. McClelland, and L.J. Rybarcyk (LANL), D. Mercer, X.Y. Chen, and D. Prout (U. Colo.), C.D. Goodman (IUCF), E. Gülmez and C.A. Whitten (UCLA), D. Marchlinski, B. Luther, and E. Sugarbaker (OSU), and J. Rapaport (Ohio U.)

#### REFERENCES

1. W.M. Alberico, A. De Pace, M. Ericson, Mikkel B. Johnson, and A. Molinari, Phys. Rev. C 38 109 (1988).
2. T.A. Carey, K.W. Jones, J.B. McClelland, J.M. Moss, L.B. Rees, N. Tanaka, and A.D. Bacher, Phys. Rev. Lett. 53, 144 (1984); L.B. Rees, J.M. Moss, T.A. Carey, K.W. Jones, J.B. McClelland, N. Tanaka, A.D. Bacher, and H. Esbensen, Phys. Rev. C 34, 627 (1986).
3. C.J. Horowitz and D.P. Murdock, Phys. Rev. C 37, 2032 (1988); C.J. Horowitz and M.J. Iqbal, Phys. Rev. C 33, 2059 (1986).
4. J.M. Moss, Phys. Rev. C 26, 727 (1982).
5. J.B. McClelland, Can. J. Phys. 65 633 (1987); in: Spin Observables of Nuclear Probes, edited by Charles J. Horowitz, Charles D. Goodman, and George E. Walker, Proceedings of the Telluride International Conference on Spin Observables of Nuclear Probes, March 14-17, 1988, Telluride, Colorado (Plenum, New York, 1988) pp. 183-193.
6. R.L. York, O.B. van Dyck, D.R. Swenson, D. Tupa, in Proceedings of the International Workshop on Polarized Ion Sources and Polarized Gas Jets, February 12-17, 1990, Tsukuba, Japan.
7. T.N. Taddeucci, C.D. Goodman, R.C. Byrd, T.A. Carey, D.J. Horen, J. Rapaport, and E. Sugarbaker, Nucl. Instrum. Methods A241, 448 (1985).
8. J.B. McClelland, D.A. Clark, J.L. Davis, R.C. Haight, R.W. Johnson, N.S.P. King, G.L. Morgan, L.J. Rybarcyk, J. Ullmann, P. Lisowski, V.R. Smythe, D.A. Lind, C.D. Zafiratos, and J. Rapaport, Nucl. Instrum. Methods A 276, 35 (1989).
9. T.N. Taddeucci, Can. J. Phys. 65, 557 (1987).
10. R.A. Arndt and L.D. Roper, Scattering Analyses Interactive Dial-In (SAID) program, Virginia Polytechnic Institute and State University (unpublished).
11. Program DWBA70, R. Schaeffer and J. Raynal (unpublished); extended version DW81 by J.R. Comfort (unpublished).
12. M.A. Franey and W.G. Love, Phys. Rev. C 31, 488 (1985).
13. H. Sakai, T.A. Carey, J.B. McClelland, T.N. Taddeucci, R.C. Byrd, C.D. Goodman, D. Krofcheck, L.J. Rybarcyk, E. Sugarbaker, A.J. Wagner, and J. Rapaport, Phys. Rev. C 35, 344 (1987).

14. R.E. Chrien, T.J. Krieger, R.J. Sutter, M. May, H. Palevsky, R.L. Stearns, T. Kozlowski, and T. Bauer, Phys. Rev. C 21, 1014 (1980).
15. G.F. Bertsch and O. Scholten, Phys. Rev. C 25 (1982) 804; H. Esbensen and G.F. Bertsch, Ann. Phys. 157, 255 (1984); H. Esbensen and G.F. Bertsch, Phys. Rev. C 32, 553 (1985).
16. R.D. Smith, Spin Observables of Nuclear Probes, edited by Charles J. Horowitz, Charles D. Goodman, and George E. Walker, Proceedings of the Telluride International Conference on Spin Observables of Nuclear Probes, March 14-17, 1988, Telluride, Colorado (Plenum, New York, 1988) pp. 15-51.
17. X.Y. Chen, L.W. Swenson, F. Farzanpay, D.K. McDaniels, Z. Tang, Z. Xu, D.M. Drake, I. Bergqvist, A. Brockstedt, F.E. Bertrand, D.J. Horen, J. Lisanntti, K. Hicks, M. Vetterli, and M.J. Iqbal, Phys. Lett. B205, 436 (1988); O. Häusser, R. Abegg, R.G. Jeppesen, R. Sawafta, A. Celler, A. Green, R.L. Helmer, R. Henderson, K. Hicks, K.P. Jackson, J. Mildemberger, C.A. Miller, M.C. Vetterli, S. Yen, M.J. Iqbal, and R.D. Smith, Phys. Rev. Lett. 61, 822 (1988); R. Fergerson, J. McGill, C. Glashausser, K. Jones, S. Nanda, Sun Zuxun, M. Barlett, G. Hoffmann, J. Marshall, and J. McClelland, Phys. Rev. C 38, 2193 (1988).
18. M. Ichimura, K. Kawahigashi, T.S. Jorgensen, and C. Gaarde, Phys. Rev. C 39, 1446 (1989).
19. M. Ichimura, private communication.